Dynamic Diffuse Double-Layer Model for the Electrochemistry of Nanometer-Sized Electrodes

Rui He, Shengli Chen,* Fan Yang, and Bingliang Wu

Department of Chemistry, Wuhan University, Wuhan 430072, P. R. China

Received: January 5, 2006

A dynamic diffuse double-layer model is developed for describing the electrode/electrolyte interface bearing a redox reaction. It overcomes the dilemma of the traditional voltammetric theories based on the depletion layer and Frumkin's model for double-layer effects in predicating the voltammetric behavior of nanometer-sized electrodes. Starting from the Nernst−Planck equation, a dynamic interfacial concentration distribution is derived, which has a similar form to the Boltzmann distribution equation but contains the influence of current density. Incorporation of the dynamic concentration distribution into the Poisson and Butler−Volmer equations, respectively, produces a dynamic potential distribution equation containing the influence of current and a voltammetric equation containing the double-layer effects. Computation based on these two equations gives both the interfacial structure (potential and concentration profiles) and voltammetric behavior. The results show that the electrochemical interface at electrodes of nanometer scales is more like an electric-double-layer, whereas the interface at electrodes larger than 100 nm can be treated as a concentration depletion layer. The double-layer nature of the electrode/electrolyte interface of nanometer scale causes the voltammetric responses to vary with electrode size, reactant charge, the value of formal redox potential, and the dielectric properties of the compact double-layer. These voltammetric features are novel in comparison to the traditional voltammetric theory based on the transport of redox molecules in the depletion layer.

1. Introduction

Electrochemical processes confined into interfacial domains of nanometer scales can be of importance in many areas including fabrication of nanomaterials and nanodevices, energy conversion, chemical sensing, and scanning probe microscopy. Since the late 1980s, electrochemistry at nanometer-sized electrodes has been the subject of extensive studies.[1−11] As well as applications in scanning probe microscopies[12−14] and measurements of fast electron-transfer rates,[6,9−11,15] electrodes of nanometer size offers novel opportunities to investigate the interfacial electrochemical reactions confined into spatial domains of nanoscales. Recently, results presented in a number of studies have shown that the voltammetric behaviors of nanometer-sized electrodes deviate significantly from the predictions of classic electrochemical theories.[1−5,7,8,16] For example, the voltammetric behavior of electrodes of submicrometer dimension upon removal of the supporting electrolyte cannot be interpreted in terms of either the conventional electromigration theories or Frumkin's double-layer effects.[1,2,4] Even in the presence of excess supporting electrolyte, the limiting currents of the steady-state polarization curves obtained at electrodes of nanometer scales for one-electron redox reactions were found to vary with redox molecules,[2] which obviously disagrees with the diffusion-based voltammetric theories. These results imply that the effects of electric fields at electrode/electrolyte interfaces on an electrochemical reaction have to be reconsidered as long as nanometer-sized electrodes are used.

The influences of the interfacial electric field on an electrode reaction are mainly described in terms of either the double-layer effect or the electromigration effect.[17] The double-layer effect, which is also called the Frumkin effect since Frumkin initially addressed the basic concept, deals with the influence of potential drop in the diffuse double-layer on the concentration of redox species at the plane of closest approach and the effective driving force of the interfacial charge transfer. The major problem in Frumkin's approach is that it is based on Gouy−Chapman's equilibrium double-layer model and that the transport of redox molecules is totally ignored. The conventional electromigration theories go to the other extremity in dealing with the interfacial electric filed effects. Most of these theories only consider the transport of redox species in the depletion layer, and the effect of the double-layer is totally ignored. Furthermore, most of the electromigration theories are based on the assumption of electroneutrality in the depletion layer.[17−19] The problems in Frumkin's approach for the double-layer effects and the conventional electromigration theories would be magnified at the electrode/electrolyte interface of nanometer scale. This is because the mass transport rates to/from nanometer-sized electrodes are very high, which, on one hand, can induce significant charge separation in the depletion layer so that the electroneutrality assumption becomes invalid and, on the other hand, can significantly break the equilibrium distribution of ions in the double-layer.

Recently, a few studies on the voltammetric theory have attempted to tackle these problems, especially the electroneutrality assumption.[7,16,20−22] The basic approach employed in these studies is to replace the electroneutrality approximation by the more rigorous Poisson equation. The studies by Smith and White[7] and Oldham and Bond[16] are particularly devoted to the voltammetric responses of nanometer electrodes through simultaneous solution of the Poisson and Nernst−Planck equations. Smith and White's numerical solution of the Nernst−

* Corresponding author. E-mail: slchen@whu.edu.cn. Phone: +86 27-68754693. Fax: +86 27-68754067.

10.1021/jp060084j CCC: $33.50
Published on Web 02/02/2006

Planck−Poisson equations demonstrated that the diffusion-based transport theories become no longer valid for predicting the voltammetric responses of electrodes of radii less than 100 nm even in the presence of an excess of a supporting electrolyte. Oldham and Bond solved the Nernst−Planck−Poisson equations in a relatively analytical way. They concluded that detectable charge separation in the depletion layer only occurs when the electrode diameter is less than 10 nm even in the absence of a supporting electrolyte. This is obviously inconsistent with the findings in recent experimental studies.[1−4] By carefully reviewing the derivation processes in Oldham and Bond's study, we found that the double-layer is actually ignored in their model. They only considered the electromigration effect although the electroneutrality approximation is avoided. Neglecting the effect of the double-layer is rather unreasonable either when a nanometer-sized electrode is used or the supporting electrolyte is absent. Smith and White's model considered both the electromigration and double-layer effects. According to their calculation, peak-shaped instead of sigmoid-shaped steady-state polarization curves would be obtained for the oxidation of a positively charged reactant (or the reduction of a negatively charged reactant) at submicrometer electrodes. So far, no experimental evidence has ever been observed to support such a prediction. Instead, sigmoid-shaped polarization curves with limiting current plateaus are usually obtained for the oxidation of cations (e.g., ferrocenylmethyltrimethylammonium cation, $TMAFc^+$)[1,4,6] or the reduction of anions (e.g., $Fe(CN)_6^{3-}$ or $IrCl_6^{2-}$)[2,3] even at very small electrodes.

The Poisson−Nernst−Planck (PNP) equations are probably the most rigorous approach on the basis of mean-field continuum theory to formulate interfacial electrochemical reactions that involve transport of redox ions in the electric field. The varied results produced by solving PNP equations for similar problems are mainly due to the diverse ways to define the boundary of an electrochemical interface in different studies. Establishing proper boundary conditions is of crucial importance in electrochemical theoretical analysis. It is the boundary conditions that define the physical nature of a specific electrochemical system, including the electrode geometries, properties of the redox reactions, and the applied electrochemical perturbations.[17] Inappropriate boundary conditions would lead to false results and conclusions even if exactly the same mathematical equations were employed. For instance, Oldham and Bond have treated the double-layer in a very different way from that in Smith and White's paper. It should also be pointed out that both of these studies have assumed that the electrode processes are transport-limited, i.e., electrochemically reversible. This allows utilization of the Nernst relationship between the electrode potential and concentrations of electroactive species as a boundary condition for solving the PNP equations. A fact that has been ignored by these researchers is that most of the electrochemical reactions would become rather irreversible at electrodes of nanometer scales due to very high mass transport rates. The Nernst relation is therefore no longer applicable.

In the face of the increasing importance of the electrochemistry at interfaces of nanometer dimensions and the wide applications of nanometer electrodes, it seems imperative to have a more accurate theoretic description of the electrochemistry of nanometer-sized electrodes. In this paper, we introduce a dynamic diffuse double-layer model to describe the electrode/electrolyte interface bearing an electrochemical reaction. In this model, the entire electrochemical interface is described as a dynamic electric double-layer; therefore, no distinction between the double-layer and the depletion layer is required. Rather than solving the PNP equation directly with a numerical method, we have derived a so-called dynamic concentration distribution equation from the Nernst−Planck equation and the Faraday law. The electrode/electrolyte interface is then formulated in a way similar to that which Gouy and Chapman used to deal with the equilibrium double-layer. The difference is that the dynamic concentration distribution equation is used instead of the Boltzmann law. A final interfacial potential distribution equation, which reduces to the traditional Poisson−Boltzmann equation when current flowing through the interface is zero, is obtained. In addition, combination of the dynamic concentration distribution equation and the Butler−Volmer equation produces a voltammetric equation containing the double-layer effects. The computation results based on this model show that the electrochemical interface becomes more like an electric-double-layer as the electrode approaches nanometer dimensions, making the traditional voltammetric theory based on the depletion layer model inappropriate. It is also shown that the structure of the compact double-layer has a crucial impact on the voltammetric responses of nanometer electrodes.

The term "dynamic diffuse double-layer" was initially used by Levich in the 1940s to describe how the diffuse double-layer may be disturbed by an electrode reaction.[23] Since he considered interfaces formed at large flat electrodes, it was shown that the influence of the double-layer on an electrode reaction is negligible in the presence of an excess of a supporting electrolyte. As will be shown in this paper, the situation at electrode/electrolyte interfaces of nanometer scales is much different.

2. Dynamic Diffuse Double-Layer Model

$$O^z + e^- = R^{z-1} \tag{1}$$

In the present study, we consider an outer-sphere one-electron reduction reaction (eq 1) at a spherical (or hemispherical) electrode. Choosing the spherical geometry simplifies the theoretical derivation without losing the generality. As the electrode size is reduced to a nanometer scale, the interfacial field would become more or less spherical despite the electrode shapes. It is assumed that the electrode is made of conductive materials so that the interfacial double-layer only extends toward the solution side and that the electrolyte solution initially contains the reactant O^z and a 1:1 ratio of a supporting electrolyte of A^+B^- with a concentration of 0.5 mol L^{-1}, which is large enough so that the conventional Frumkin double-layer effect can be avoided and a further increase of the supporting electrolyte concentration would result in little change on the double-layer structure. For simplicity, we also make the following assumptions: the counterion accompanying the reactant O^z is either A^+ or B^- depending on the sign of the reactant charge z; the initial concentration ratio between the reactant A_zO (or OB_z) and the supporting electrolyte is 0.01, which ensures a negligible contribution of electromigration of redox species to the voltammetric responses according to traditional electrochemical theories; none of the ions in the solution specifically adsorbs on the electrode surface and all the ions have the same plane of closest approach (PCA, which is also called the outer Helmholz plane and is denoted as OHP) so that no charge resides in the compact part of the double-layer; the plane of electron transfer (PET) coincides with the PCA, i.e., the electron transfer occurs at $r = r_0 + \mu$, where r is the radial coordinate originating from the center of the spherical electrode, r_0 is the electrode radius, and μ is the thickness of the compact double-layer; the potentials are measured with

respect of that in the bulk solution, which is assumed to be equivalent to the potential of zero charge (PZC).

The way we model the dynamic electrode/electrolyte interface is similar to that which Gouy and Chapman used to treat the equilibrium electrochemical interface. Gouy−Chapman's equilibrium double-layer model is based on the Boltzmann distribution of ions (eq 2) and the Poisson equation (eq 3).

$$c_j = c_j^{\mathrm{b}} \mathrm{e}^{-(z_j F/RT)\varphi} \tag{2}$$

$$\nabla^2 \varphi = -\frac{\rho}{\epsilon \epsilon_0} \tag{3}$$

In eqs 2 and 3, c_j and c_j^{b} are the local and bulk concentration of ion j, respectively; z_j is its charge; φ is the local potential; ϵ and ϵ_0 are the local dielectric constant and the permittivity of a vacuum; $\rho = \sum z_j c_j$ is the local charge density; and F, R, and T have their usual meanings. Combining eqs 2 and 3 produces the well-known *Poisson−Boltzmann* equation, that is

$$\nabla^2 \varphi = -\frac{1}{\epsilon \epsilon_0} \sum_j c_j^{\mathrm{b}} \mathrm{e}^{-(z_j F/RT)\varphi} \tag{4}$$

Solving eq 4 gives a gradient potential profile in the diffuse double-layer.

The major difference of a dynamic electrochemical interface from the equilibrium one is that there is net movement of ions through the interface due to interfacial reactions. Thus, the Boltzmann law that describes the equilibrium distribution of ions becomes inappropriate. The transport of ions in an electric field is generally described by the Nernst−Planck equation, according to which the flux J (mol cm^{-2} s^{-1}) of the ion j is

$$J_j = -D_j \nabla c_j - \frac{z_j F}{RT} D_j c_j \nabla \varphi \tag{5}$$

where D_j refers to the diffusion coefficient of ion j. As the steady state has been reached,

$$\frac{\partial c_j}{\partial t} = -\nabla J_j = 0 \tag{6}$$

In spherical coordinates,

$$\nabla J_j = \frac{\mathrm{d}J_j}{\mathrm{d}r} + \frac{2}{r} J_j = \frac{1}{r^2} \frac{\mathrm{d}}{\mathrm{d}r}(r^2 J_j) \tag{7}$$

It is easily recognized from eqs 6 and 7 that

$$r^2 J_j = \text{const} \tag{8}$$

According to the mass conservation and Faraday laws, we have the following equation at PET

$$(J_j)_{r=r_0+\mu} = -m_j \frac{i}{F} \tag{9}$$

where i is the current density flowing through the electrode/electrolyte interface, m_j is a integer constant and takes values of -1, $+1$, and 0 for species R^{z-1}, O^z, and inert electrolyte species (A^+ and B^-), respectively, if the reduction current is defined as positive. Combining eqs 5, 8, and 9 gives

$$D_j \frac{\mathrm{d}c_j}{\mathrm{d}r} + \frac{z_j F}{RT} D_j c_j \frac{\mathrm{d}\varphi}{\mathrm{d}r} = m_j \frac{(r_0+\mu)^2 i}{r^2 F} \tag{10}$$

We may solve eq 10 to obtain current-density dependent concentration profiles for species j. Before doing so, it will be useful to make the spatial coordinate r dimensionless by letting $p = (r_0 + \mu)/r$, which enables the problem of solving equations in the infinite range of $(r_0 + \mu) \le r \le \infty$ to be replaced by that in the finite interval of $1 \ge p \ge 0$. Some other dimensionless variables will lead to further notational economy; they are the following: the dimensionless potential, $\phi = F\varphi/RT$; the dimensionless concentration, $c_j^* = c_j/c_{\mathrm{O}}^{\mathrm{b}}$; the dimensionless current density, $i^* = i/i_{\mathrm{dL}}$, in which $i_{\mathrm{dL}} = FD_{\mathrm{O}}c_{\mathrm{O}}^{\mathrm{b}}/(r_0+\mu)$ corresponds to the limiting current density for the reduction of O^z to R^{z-1} under pure diffusion control. It should be noticed that i_{dL} thus defined is different from the limiting diffusion current density in conventional voltammetric theories. The latter is defined as $FD_{\mathrm{O}}c_{\mathrm{O}}^{\mathrm{b}}/r_0$, in which the thickness of compact double-layer μ is ignored in the reaction coordinate. For simplicity, we also assume that O and R have the same diffusion coefficient D. Thus, eq 10 reduces to the following dimensionless form,

$$\frac{\mathrm{d}c_j^*}{\mathrm{d}p} + z_j c_j^* \frac{\mathrm{d}\phi}{\mathrm{d}p} = -m_j i^* \tag{11}$$

Solving eq 11 with boundary conditions that $c_{\mathrm{O}}^* = 1$ and $c_{\mathrm{R}}^* = c_{\mathrm{R}}^{\mathrm{b}}/c_{\mathrm{O}}^{\mathrm{b}}$ at $p = 0$ gives

$$c_j^* = \mathrm{e}^{-z_j\phi}(c_j^{\mathrm{b}}{}^* - i^* \Omega_j) \tag{12}$$

where

$$\Omega_j = m_j \int_0^p \mathrm{e}^{z_j\phi}\, \mathrm{d}p \tag{13}$$

The derivation details of eq 12 are given in Appendix A. This equation represents a dynamic distribution of ionic species at an interface where a redox reaction is proceeding since the influence of current density (i.e., the reaction rate) is included. Equation 12 will becomes the dimensionless Boltzmann equation when $m_j = 0$. This says that the local electrostatic equilibrium distribution of inert electrolyte species is maintained even though there is a current flowing through the electrode/electrolyte interface. However, the distribution of redox species of O^z and R^{z-1} is altered due to the occurrence of interfacial reactions. The deviation from the equilibrium profiles depends on the current density. The larger the current density, the more the redox species deviate from a Boltzmann distribution. As the current density goes to zero, the Boltzmann distribution is recovered.

Similar to Gouy and Chapman's approach for the equilibrium double-layer, we can combine the derived dynamic distribution equation and the Poisson equation to obtain a dynamic interfacial equation. The Poisson equation has the following dimensionless form,

$$p^4 \frac{\mathrm{d}^2\phi}{\mathrm{d}p^2} = -(r_0+\mu)^2 \kappa^2 \sum z_i c_i^* \tag{14}$$

where

$$\kappa^2 = \left(\frac{\epsilon \epsilon_0 RT}{F^2 2 c_{\mathrm{O}}^{\mathrm{b}}}\right)^{-1} \tag{15}$$

The reciprocal of κ has the dimension of thickness and is called the Debye−Hückel length. Substitution of eq 12 into eq 14 yields

$$\frac{d^2\phi}{dp^2} = -\frac{(r_0+\mu)^2\kappa^2}{p^4}[\sum(z_j c_j^{b*} e^{-z_j\phi}) + i^*\sum\Omega_j z_j e^{-z_j\phi}] \quad (16)$$

It can be seen that eq 16 will reduce to the dimensionless Poisson−Boltzmann (PB) equation when the current density is zero. Similar to the PB equation, that is, the basic interfacial equation under equilibrium, eq 16 is a characteristic equation to describe the dynamic electrochemical interface where an interfacial reaction is taking place. Unlike the PB equation, eq 16 alone is insufficient to reveal the interfacial properties and behaviors since it contains an additional unknown variable, the current density. It is well-known that the current−potential dependence can be described by the Butler−Volmer equation, which has the following dimensionless form

$$i^* = \frac{k^0(r_0+\mu)}{D}[c_O{}^{s*} e^{-\alpha(E-\phi_{PET}-E^{0\prime})} - c_R{}^{s*} e^{\beta(E-\phi_{PET}-E^{0\prime})}] \quad (17)$$

In eq 17, k^0 is the standard rate constant of redox reaction of eq 1 at formal potential $E^{0\prime}$, and α and β are the transfer coefficients. E is the potential value at the electrode surface. ϕ_{PET}, $c_O{}^{s*}$, and $c_R{}^{s*}$ are the potential, concentration of O^z, and concentration of R^{z-1} at PET, respectively. All the concentrations and potentials are in their dimensionless forms. The difference between eq 17 and the conventional Butler−Volmer equation is that the potential drop in the diffuse double-layer (ϕ_{PET}) is incorporated in eq 17. This is similar to Frumkin's approach to correct the double-layer effects. The main problem in the Frumkin model for double-layer effects is that the concentrations and diffuse double-layer potential are treated according to Gouy−Chapman's equilibrium double-layer theory.[17] For instance, $c_O{}^{s*}$ and $c_R{}^{s*}$ are determined using the Boltzmann equation. This is obviously problematic as an interfacial reaction is taking place. Instead of using the Boltzmann distribution law, we can substitute $c_O{}^{s*}$ and $c_R{}^{s*}$ with eq 12 by setting $p = 1$. Considering that $c_O{}^{b*} = 1$ and $c_R{}^{b*} = 0$, we have

$$i^* = \frac{1}{\frac{1}{\lambda}e^{\alpha(E-E^{0\prime})}e^{(z-\alpha)\phi_{PET}} + \Lambda_O + \Lambda_R e^{(E-E^{0\prime})}} \quad (18)$$

in which $\lambda = k^0(r_0+\mu)/D$ and $\Lambda_j = \int_0^1 e^{z_j\phi}\,dp$. Equation 18 is a voltammetric equation containing the double-layer effects. The traditional steady-state voltammetric equation without considering the double-layer effects is

$$i^* = \frac{1}{\frac{1}{\lambda}e^{\alpha(E-E^{0\prime})} + 1 + e^{(E-E^{0\prime})}} \quad (19)$$

which can be derived by combining the Butler−Volmer equation with Fick's diffusion law.[17,24]

Thus, eqs 16 and 18 are the final equations of the dynamic double-layer model. Simultaneously solving these two equations with appropriate boundary conditions will be able to give the potential profiles at and the current density flowing through the electrode/electrolyte interface.

Since eq 16 is a second-order differential equation about the potential, two boundary conditions related to the potential are required to solve it. We have assumed that the plane of closest approach for all the redox molecules is at the PET; thus, the two boundaries are the bulk solution ($p = 0$) and the PET ($p = 1$), respectively. The boundary condition in the bulk solution is

$$\phi_{p=0} = 0 \quad (20)$$

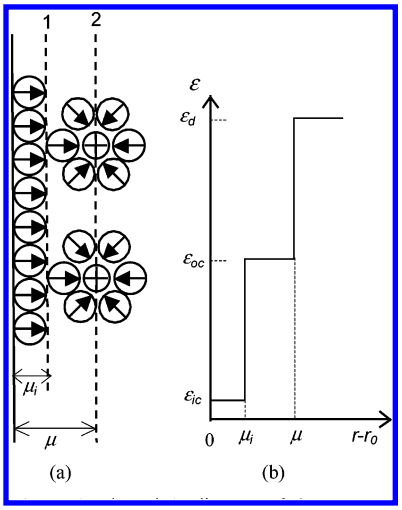

Figure 1. Schematic diagram of the compact double-layer (a) and the dielectric variation in the interfacial region (b).

The potential at the boundary of the PET ($p = 1$) depends on the electrode potential E at the surface and the potential drop in the compact double-layer. To obtain the potential drop in the compact double-layer, a fairly detailed model of the double-layer and its dielectric properties must be specified. It is generally recognized that the dielectric permittivity changes with distance from the electrode surface in the interfacial region.[25−27] For simplicity, we assume that the compact double-layer can be divided into two regions (see Figure 1a): the inner part that is composed of the first layer of the solvent molecules bound to the electrode surface and the outer part that spans from the outer edge (dotted line 1 in Figure 1a) of the inner part to the plane of closest approach of ions (dotted line 2 in Figure 1a).[17,25,27] We also assume that the dielectric permittivity is uniform within each region of the double-layer but that it has different values in different regions (Figure 1b). Such assumptions enable us to correlate the potential at the PET, ϕ_{PET}, to the electrode potential E as

$$\phi_{PET} = E - \frac{(r_0+\mu)^2}{(r_0+\mu_i)}\left(\frac{\mu_i\epsilon_d}{r_0\epsilon_{ic}} + \frac{(\mu-\mu_i)\epsilon_d}{(r_0+\mu)\epsilon_{oc}}\right)\left(\frac{d\phi}{dr}\right)_{PET} \quad (21)$$

In eq 21, ϵ_{ic}, ϵ_{oc}, and ϵ_d are the effective dielectric constants of the inner part of the compact double-layer, the outer part of the compact double-layer, and the diffuse double-layer, respectively and μ_i is the thickness of the inner part of the compact double-layer. The derivation details of eq 21 are shown in Appendix B.

Equations 16 and 18 are solved numerically with the boundary conditions of eqs 20 and 21 according to the method and parameters given in Appendix C.

3. Results and Discussion

3.1. Electric-Double-Layer Nature of Electrochemical Interfaces at Electrodes of Nanometer Scales. The dimensionless current density i^* given by simultaneous solution of eqs 16 and 18 is actually the normalized value of the real current density by the limiting current density due to diffusion, i_{dL}. Thus, the limiting value of i^* should be equal to one if the electrode reaction is controlled purely by the diffusion of redox species. Figure 2 shows the computed steady-state i^*-E curves corresponding to the reaction of eq 1 with $z = -1$ at electrodes of different sizes. The numbers inserted in the figure refer to the electrode radii. It can be seen that the i^*-E curves have sigmoid

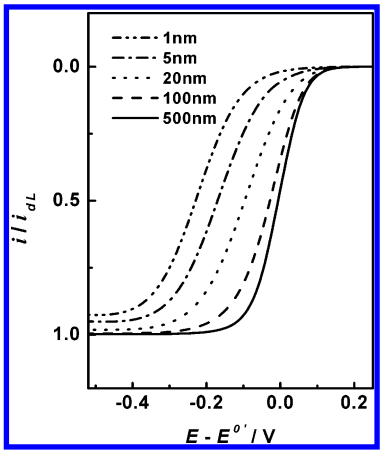

Figure 2. Theoretical steady-state voltammetric curves corresponding to the reduction of 5×10^{-3} mol L^{-1} O^z with $z = -1$ at electrodes of a variety of sizes. The parameters are the following: $k^0 = 1.0$ cm s^{-1}, $D = 1 \times 10^{-5}$ cm s^{-2}, $\alpha = \beta = 0.5$, $E^{0\prime} = 0$, (the concentration of supporting electrolyte) $c_{AB} = 0.5$ mol L^{-1}.

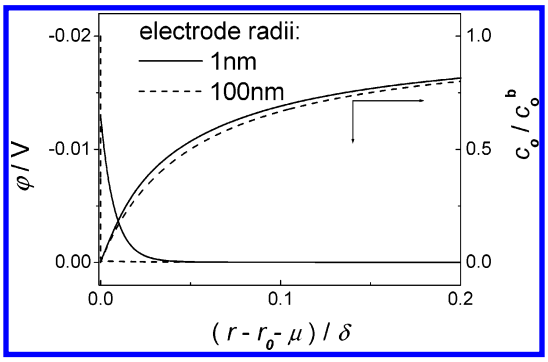

Figure 3. Potential and reactant concentration profiles in the interfacial region. The conditions and parameters are the same as those for Figure 2.

shapes regardless of the electrode size. At electrodes larger than 100 nm, the limiting current density is almost the same as the diffusion-controlled limiting current density i_{dL}, i.e., $i^* = 1$. This indicates that the influence of the electric field on the voltammetric behavior at electrodes larger than 100 nm is negligible. However, the value of the limiting current density deviates gradually from i_{dL} as the electrode radius goes below 100 nm. The smaller the electrode size, the more the limiting current density deviates from i_{dL}.

Figure 3 shows the distribution of the potential and the reactant concentration in the interfacial region at electrodes of 100 nm (dash line) and 1 nm (solid line) in radii, respectively, as $E - E^{0\prime} = -0.5$ V where the limiting current is reached. The potential distribution can be obtained simultaneously with the current density by solution of eqs 16 and 18. The concentration distribution is then obtained according to eq 12 with the calculated potential distribution and the current density. The *x*-axis in Figure 3 represents the distance from the PET normalized by a thickness parameter δ, which is measured from the PET to the location where the concentration of reactant O^z reaches 95% of its bulk value. We may consider δ as the thickness of the entire interfacial region. It can be seen that the interfacial potential distribution at an electrode of 100 nm occurs in a very narrow region that is negligible in the entire interface. The penetration of the electric field into the concentration field is almost unseen (less than 0.01%). This implies that the influence of the interfacial electric field on the voltammetric responses of electrodes larger than 100 nm should be negligible. Whereas, significant overlap between potential gradient and

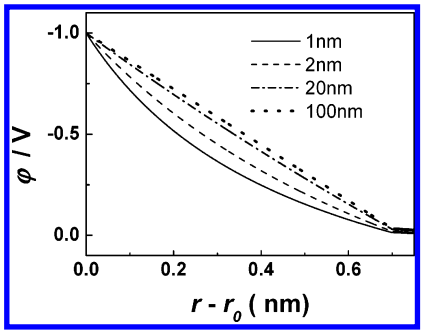

Figure 4. Potential distribution inside the compact double-layer at electrodes of different sizes. The electrode potential $E = 0.1$ V. The numbers inserted in the figure refer to the radii of electrodes.

concentration gradient is seen at an electrode of 1 nm in radius; therefore, pronounced effects of the electric field on the voltammetric responses are expected. Thus, the potential and concentration profiles in Figure 3 can explain the deviation of the limiting current density from i_{dL} at electrodes smaller than 100 nm shown in Figure 2 well, i.e., the pronounced penetration of the electric field into the concentration field makes the transport of redox molecules deviate from pure diffusion behavior as the electrode size approaches nanometer scale. At large electrodes, the interface is more like a concentration depletion layer, whereas it is more close to an electric-double-layer at an electrode of nanometer scale. The electric-double-layer nature of the interface at nanometer electrodes may raise some voltammetric features that are unseen in the voltammetric behaviors of conventional large electrodes.

It should be pointed out that the voltammetric behaviors of electrodes having radii of 1 nm or less would not be affected by the electrostatic double-layer effects addressed above only. The finite molecule size of ions may play a significant role in the voltammetric responses of such small electrodes. As discussed by Smith and White,[7] the point-charge assumption of ions would unrealistically overestimate the screening of the electrode charge by the inert ions, which tends to diminish the effects of the interfacial electric field. Thus, considering the finite molecule size of ions, the double-layer effects should be more pronounced than those predicted by the present model.

3.2. Effect of Electrode Size. The double-layer nature of the interface makes the intrinsic interfacial properties and behavior become size-dependent. This has been depicted in Figures 2 and 3, which show that the voltammetric behaviors and interfacial structures are electrode-size dependent as $r_0 < 100$ nm. The electrode size effects are actually implied by eq 21 that defines the boundary of the diffuse double-layer. As mentioned in the Introduction, the boundary conditions have a crucial impact on the computation results. It is seen from eq 21 that the electrode size becomes significant only when r_0 is close to μ. Otherwise, as $r_0 \gg \mu$, eq 21 becomes

$$\phi_{PET} = E - \left(\frac{\mu_i \epsilon_d}{\epsilon_{ic}} + \frac{(\mu - \mu_i)\epsilon_d}{\epsilon_{oc}}\right)\left(\frac{d\phi}{dr}\right)_{PET} \qquad (22)$$

in which the electrode size effect disappears. As shown in Figure 4, the structure of the compact double-layer also depends on the electrode size. For an electrode having a radius larger than 100 nm, the potential distributes itself linearly in the compact double-layer, which has been generally recognized for conventional electrodes of large scales.[17,27] As the electrode becomes smaller than 100 nm, however, the potential distribution gradually becomes curved and varies with electrode size.

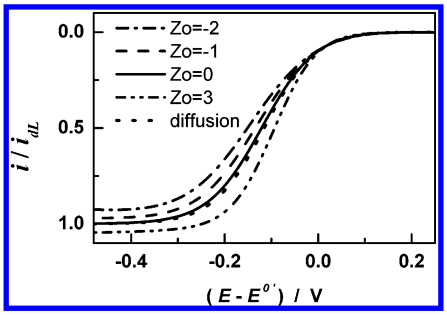

Figure 5. Steady-state voltammetric curves for the reduction of differently charged reactants at an electrode of 10 nm. The other conditions and parameters are the same as those for Figure 2.

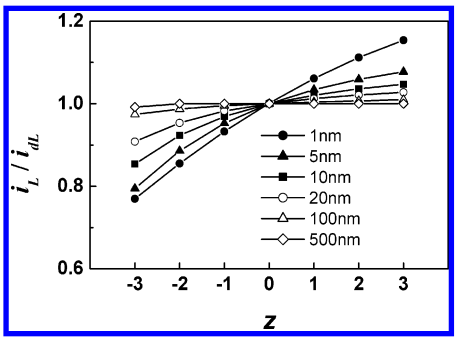

Figure 6. Ratio between the limiting current density predicated by the dynamic diffuse double-layer model and that calculated according to eq 19 for reduction of variously charged reactants at electrodes having different sizes. The other conditions and parameters are the same as those for Figure 2.

3.3. Effect of Reactant Charge. As indicated by eq 18, the effects of the double-layer cause the current−potential relation at nanometer electrodes to depend on the charge z carried by the reactant. This is manifested by the voltammetric curves for the reduction of differently charged reactants at an electrode of 10 nm in Figure 5. The deviation from the diffusion behavior becomes more pronounced for a reactant with a higher charge. The reduction of a negatively charged reactant and a positively charged reactant are inhibited and enhanced, respectively. For the reduction of a neutral reactant, the limiting current is almost the same as i_{dL}. However, the whole voltammetric curve does not necessarily overlap with the diffusion-controlled one calculated according to eq 19 (dotted line). Although the transport of the neutral reactant is not affected by the interfacial electric field, the transport and profile of the product is still affected. In addition, the potential drop in the diffuse part of the double-layer modifies the effective driving force for the charge-transfer step, as suggested by Frumkin's double-layer effects.[17]

Figure 6 summarizes the effects of the electrode size and reactant charge on the ratio between the real limiting current density i_L and the limiting diffusion current density i_{dL}. It can be seen that the difference between i_L and i_{dL} is negligible when the electrode radius is larger than 100 nm, but it becomes larger and larger with decreased electrode size and increased reactant charge.

3.4. Effect of the Compact Double-Layer Structure. It is noticed that the differences between i_L and i_{dL} calculated in this study are much less than that reported by Smith and White in a recent study on voltammetric theories of nanometer electrodes,[7] although we have chosen the same studying system, a one-electron redox process of 5 mM reactant in the presence of a 1:1 supporting electrolyte of 0.5 M, and have employed the same theoretical approach, i.e., Nernst−Planck−Poisson equations. According to Smith and White's calculation, the limiting current density for the reduction of reactants with a charge of +1 will be enhanced by 50% at an electrode of 1 nm in radius. The results in this study show an enhancement of about 5%. Even for the reduction of reactants with a charge of +3, the enhancement of i_L is less than 20%. In addition, Smith and White's study indicated that the reduction of a negatively charged reactant (or oxidation of a positively charged reactant) at electrodes of submicrometer radii would be greatly inhibited so that a peak-shaped rather than sigmoid-shaped $i-E$ curve would be obtained. The results in the present study have shown that the reduction of negatively charged reactants on very small electrodes still exhibits sigmoid-shaped polarization curves.

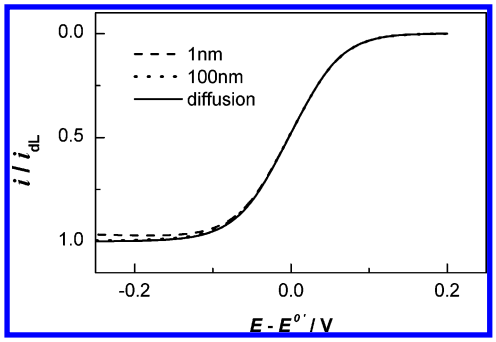

Figure 7. Theoretical voltammetric curves for $k^0 = 1000$ cm s^{-1}. The other conditions and parameters are the same as those for Figure 2.

There are mainly two differences between the theoretical treatment in the present study and that by Smith and White. First, we use the Butler−Volmer equation rather than the Nernst relationship to correlate the electrode potential and concentrations of redox molecules at the PET. This causes the voltammetric behavior for a redox reaction with $k^0 = 1$ cm s^{-1} to become totally irreversible at nanometer electrodes. Figure 7 gives the voltammetric responses for a one-electron reduction reaction with $k^0 = 1000$ cm s^{-1} so that $k^0 r_0/D = 10$, which means that the reaction is totally reversible. In such a case, the Butler−Volmer equation is actually equivalent to the Nernst equation. It can be seen that the limiting current density on i^*-E curves for electrodes of the same size in Figure 7 shows less deviation from the diffusion behavior than that for $k^0 = 1$ cm s^{-1}, as shown in Figure 2. This says that the assumption of reversibility would not enhance the deviation of voltammetric responses from diffusion-controlled behavior.

A second difference between the current study and that by Smith and White is the compact double-layer structure that is used to establish the boundary condition at the PET. Smith and White treated the compact double-layer as a uniform dielectric of 0.2 nm in thickness with the same dielectric constant as that in bulk solution, e.g., 78. Such a compact double-layer model is unreasonable in a few aspects. It is generally recognized that the dielectric permittivity is not uniform in the double-layer due to the interfacial electric field.[26,27] In the absence of specific adsorption, the inner part of the compact double-layer is made up of a layer of highly oriented solvent molecules with a dielectric constant of about 6, which is much lower than the value in bulk solution.[27] The nonspecific adsorbed ions usually approach the electrode with their solvent shell or other ligands and cannot penetrate into the first solvent layer (see Figure 1a). The dielectric constant of this layer is between that of the inner solvent layer and the bulk solution. The thickness of the compact double-layer may be approximately estimated using[27,28]

$$\mu = 2r_w + \sqrt{3}r_w + r_i \qquad (23)$$

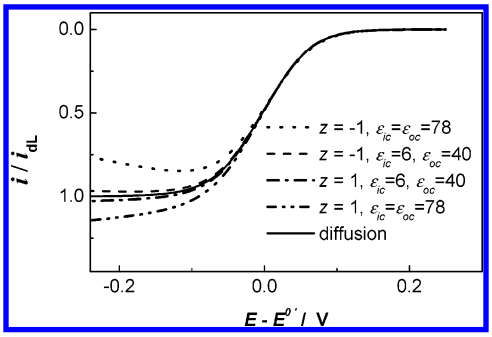

Figure 8. Theoretical voltammetric responses of an electrode of 1 nm in radius calculated based on the assumption of different dielectric properties in the compact double-layer. The other conditions and parameters are the same as those for Figure 7.

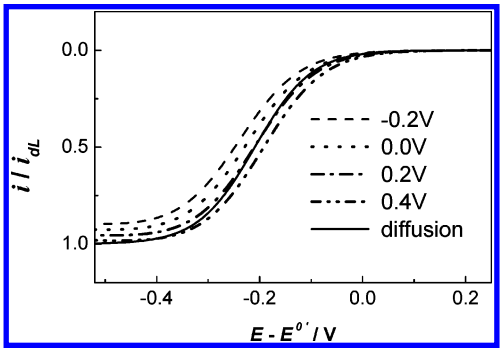

Figure 9. Theoretical voltammetric responses of an electrode of 1 nm in radius for reactions with different redox formal potentials (shown by the numbers inserted). The other conditions and parameters are the same as those for Figure 2.

where r_w is the radius of water molecules and r_i is the radius of the ions that carry the charges to compensate the electrode charge. The thickness of the inner region of the compact double-layer can be considered to equal the hard sphere diameter of water, 0.29 nm.[27,28] The outer part of compact double-layer can be considered to consist of the thickness of the solvent shell and half of the ion diameter. As shown in Figure 8, voltammetric curves calculated for the reduction of an anion with a charge of -1 using eqs 16 and 18 with boundary condition based on the assumption that the compact double-layer has a uniform dielectric constant of 78 does show curved shapes. The low dielectric constant inside the compact double-layer causes the potential to mainly drop in the compact double-layer. If one ignores it, the diffuse double-layer potential will be overestimated; therefore, the double-layer effects will be overestimated.

3.5. Effect of the Redox Formal Potential. The double-layer nature of the interface at an electrode of nanometer scale would result in another particular behavior: the votammetric response would depend on the value of the redox formal potential. This is depicted by the polarization curves at electrodes of 1 nm for redox reactions having different formal potentials shown in Figure 9. For the reduction of a negatively charged reactant, a positive shift of $E^{0\prime}$ enhances the reaction rate, as indicated by the increased limiting current density. Such a dependence of voltammetric responses on $E^{0\prime}$ does not occur on large electrodes, as indicated by the voltmetric curves for different $E^{0\prime}$ at an electrode of 100 nm shown in Figure 10. The influence of $E^{0\prime}$ on the voltammetric responses of nanoelectrodes originates from the variation of the charge density on the electrode surface with the departure of the electrode potential from the PZC, which affects the distribution of the potential and concentration of ions in the double-layer. At electrodes larger than 100 nm, the electrode reaction with $k^0 =$ 1 cm s^{-1} would become reversible and the influence of the double-layer on the interfacial reaction kinetics is negligible in the presence of an excess of a supporting electrolyte. For redox reactions with lower k^0 values or in the absence of a supporting electrolyte, a dependence of voltammetric response on $E^{0\prime}$ would also occur on large electrodes.

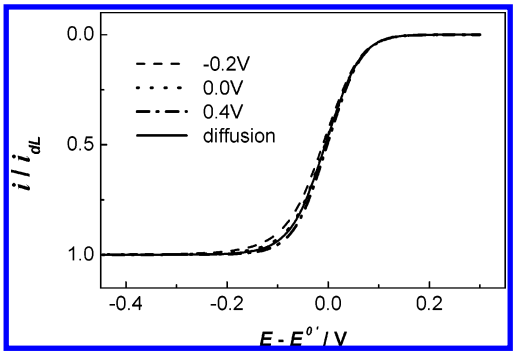

Figure 10. Theoretical voltammetric responses of an electrode of 100 nm in radius for reactions with different redox formal potentials (shown by the numbers inserted). The other conditions and parameters are the same as those for Figure 2.

As well as the limiting current density, the double-layer nature of the interface at nanometer electrodes also affects the shape of the voltammetric curves, e.g., the half wave potentials. We will give a detailed discussion on this issue in a separate paper.

4. Conclusion

A dynamic diffuse double-layer model has been established to describe electrochemical interfaces bearing a redox reaction. The model consists of a dynamic potential distribution equation containing the influence of current and a voltammetric equation containing the influence of the double-layer. It is shown that this model can well predicate the voltammetric responses of electrodes of various sizes. The computed results according to this model indicate that the steady-state polarization curves corresponding to outer-sphere redox reactions have sigmoid shapes even at nanometer electrodes. However, the limiting current and the half wave potential on the voltammetric curves change with electrode sizes, reactant charges, dielectric properties of the double-layer, and the redox formal potentials. These particular voltammetric behaviors seen on nanometer electrodes disappear from the voltammetric responses at electrodes larger than 100 nm calculated with the same model. It is shown that the anomalous voltammetric features of nanometer-sized electrodes are due to the electric-double-layer nature of the electrode/electrolyte interfaces.

Acknowledgment. This work is financially supported by the National Natural Science Foundation of China (NSFC No. 20443009), the Research Fund for the Doctoral Program of Higher Education, State Education Ministry of China (RFDP No. 20050486025), and the Scientific Research Foundation for the Returned Overseas Chinese Scholars, State Education Ministry of China (ROCS No. 2005-383).

Appendix A: Derivation of Equation 12

Equation 11 can be transformed into the following form by setting $c_j^* = Q_1 Q_2$,

$$Q_1\left(\frac{dQ_2}{dp} + z_j Q_2 \frac{d\phi}{dp}\right) + Q_2 \frac{dQ_1}{dp} = -m_j i^* \qquad \text{(A1)}$$

where Q_1 and Q_2 are functions of p. We can chose Q_2 so that

$$\frac{dQ_2}{dp} + z_j Q_2 \frac{d\phi}{dp} = 0 \quad \text{(A2)}$$

This requires

$$Q_2 = e^{-z_j\phi} \quad \text{(A3)}$$

Combining eqs A1, A2, and A3 leads to

$$e^{-z_j\phi}\frac{dQ_1}{dp} = -m_j i^* \quad \text{(A4)}$$

We then have

$$Q_1 = Q_1{}^b - m_j i^* \int_0^p e^{z_j\phi}\, dp \quad \text{(A5)}$$

where $Q_1{}^b$ refers to the value of Q_1 when $p = 0$ (bulk solution). Thus, c_j^* can be expressed as

$$c_j^* = e^{-z_j\phi}[Q_1{}^b - m_j i^* \int_0^p e^{z_j\phi}\, dp] \quad \text{(A6)}$$

Considering that $\phi = 0$ and $c_j^* = c_j{}^{b*}$ when $p = 0$, we have

$$c_j^* = e^{-z_j\phi}[c_j{}^{b*} - m_j i^* \int_0^p e^{z_j\phi}\, dp] \quad \text{(A7)}$$

Appendix B: Derivation of Equation 21

According to the Gaussian law, the total charge within any enclosure equals the outward normal electric field strength integrated over the boundary surface of the enclosure multiplied by the local permittivity. Due to the fact that there is no charge in the compact double-layer, the total charge within any enclosures that have radii of $r_0 \le r \le .\ r_0 + \mu$ equals the charge amount at the electrode surface q. Thus,

$$-4\pi\, r^2 \epsilon\epsilon_0 \frac{d\phi}{dr} = q \quad \text{(B1)}$$

Since we have assumed that ϵ is constant within a specific region of the double-layer, eq B1 may be integrated in the inner region of the compact double-layer as

$$-\frac{q}{4\pi\epsilon_0\epsilon_{ic}}\int_{r_0}^{r_0+\mu_i}\frac{1}{r^2}\,dr = \int_E^{\phi_{ihp}} d\phi \quad \text{(B2)}$$

so,

$$\phi_{ihp} = E - \frac{q}{4\pi\epsilon_{ic}\epsilon_0}\left(\frac{1}{r_0} - \frac{1}{r_0+\mu_i}\right) \quad \text{(B3)}$$

Similarly,

$$\phi_{ohp} = \phi_{ihp} - \frac{q}{4\pi\epsilon_{oc}\epsilon_0}\left(\frac{1}{r_0+\mu_i} - \frac{1}{r_0+\mu}\right) \quad \text{(B4)}$$

where ϕ_{ihp} and ϕ_{ohp} refer to the potential at the inner Helmholz plane (IHP) and OHP, respectively. Replacing ϕ_{ihp} in eq B4 with eq B3 gives

$$\phi_{ohp} = E - \frac{q}{4\pi\epsilon_{ic}\epsilon_0}\left(\frac{1}{r_0} - \frac{1}{r_0+\mu_i}\right) - \frac{q}{4\pi\epsilon_{oc}\epsilon_0}\left(\frac{1}{r_0+\mu_i} - \frac{1}{r_0+\mu}\right) \quad \text{(B5)}$$

We can imagine a spherical Gaussian enclosure that is located just outside of the OHP but does not include any charge in the diffuse double-layer. For such an enclosure, eq B1 becomes

$$-4\pi(r_0+\mu)^2\epsilon_d\epsilon_0\left(\frac{d\phi}{dr}\right)_{ohp} = q \quad \text{(B6)}$$

Replacing q in eq B5 with eq B6 leads to

$$\phi_{ohp} = E - \frac{(r_0+\mu)^2\epsilon_d}{\epsilon_{ic}}\left(\frac{1}{r_0} - \frac{1}{r_0+\mu_i}\right)\left(\frac{d\phi}{dr}\right)_{ohp} - \frac{(r_0+\mu)^2\epsilon_d}{\epsilon_{oc}}\left(\frac{1}{r_0+\mu_i} - \frac{1}{r_0+\mu}\right)\left(\frac{d\phi}{dr}\right)_{ohp} \quad \text{(B7)}$$

Since we have assumed that the PET coincides with the OHP, eq 21 is actually equivalent to eq B7 by replacing the subscript ohp with PET.

Appendix C: Numerical Method for Solving Equations 16 and 18

Equation 16 is solved numerically in the p-domain using the finite-difference method. Second-order, center-finite difference formulas are employed to discretize eq 16 and the boundary conditions. To do so, the entire p-domain [0, 1] was divided into 2 subdomains: $[0, (r_0+\mu)/(r_0+\mu+A/\kappa_1)]$ and $[(r_0+\mu)/(r_0+\mu+A/\kappa_1), 1]$, where A is a constant that is chosen to make sure that the potential at $p = (r_0+\mu)/(r_0+\mu+A/\kappa_1)$ is negligibly small compared to the electrode potential, e.g., 10^{-5} V. The term κ_1 is the reciprocal of the Debye length calculated with the total concentration of ions in the solution, that is

$$\kappa_1 = -\left(\frac{\epsilon_d\epsilon_0 RT}{2F^2 c}\right)^{-1/2} \quad \text{(C1)}$$

where

$$c = c_O{}^b + c_R{}^b + c_A{}^b + z c_B{}^b \quad \text{(C2)}$$

The subdomain of $[0, (r_0+\mu)/(r_0+\mu+A/\kappa_1)]$ is equally divided by N_1 nodes in the p-domain with node 1 corresponding to $p = 0$ (bulk solution) and node N_1 located at $p = (r_0+\mu)/(r_0+\mu+A/\kappa_1)$. The subdomain of $[(r_0+\mu)/(r_0+\mu+A/\kappa_1), 1]$ is unevenly divided by N_2 nodes where the node $N_1 + m$ is located at

$$p_{N_1+m} = \frac{r_0+\mu}{r_0+\mu+\frac{A}{\kappa_1}\left(1-\frac{m}{N_2}\right)} \quad \text{(C3)}$$

This will result in an even node spacing in the real r-domain. Such a dividing strategy is used for better computation accuracy. According to the definition of dimensionless distance p, we may have

$$\Delta p \approx -\frac{r_0+\mu}{r^2}\Delta r \quad \text{(C4)}$$

It can be seen that the Δr value becomes larger at smaller r for a specific Δp value. Thus, evenly dividing the p-domain will render the real spacing in the r-domain near the PET very large, therefore resulting in large computation inaccuracy. To gain the necessary accuracy, the node spacing Δp has to be very small; this greatly increases the computation time. If the inner subdomain is divided according to eq C3, both the computation accuracy and computation time requirements can be well satisfied. The computing procedure is as follows: First, eq 16

is solved by setting $i^* = 0$. This will produce the equilibrium potential distribution at a specific electrode potential. The resulting potential profile can be used to obtain a current density and concentration profiles according to eqs 18 and 12, respectively. The thus-obtained current density and concentration profiles are then used to solve eq 16 to produce a potential profile, which is used to obtain new current density and concentration profiles according to eqs 18 and 12. Then, a new potential profile is obtained by solving eq 16. Such a computation cycle is repeated until the current density and potential profile show negligible differences from the last calculation cycle. In the computation, we have set $N_1 = 1000$ and $N_2 = 5000$. The computation is performed with home-written program codes in Matlab. The parameters used in the computation are: $\alpha = \beta = 0.5$, $\mu_i = 2r_w = 0.29$ nm, $\epsilon_{ic} = 6$, $\epsilon_{oc} = 40$, $\epsilon_d = 78$, $T = 298$ K, $E^{0\prime} = 0$ unless stated, $D = 1 \times 10^{-5}$ cm s^{-2}.

References and Notes

(1) Watkins, J. J.; White, H. S. *Langmuir* **2004**, *20*, 5474−5483.

(2) Chen, S. L.; Kucernak, A. *J. Phys. Chem. B* **2002**, *106*, 9396−9404.

(3) Chen, S. L.; Kucernak, A. *Electrochem. Commun.* **2002**, *4*, 80−85.

(4) Conyers, J. L.; White, H. S. *Anal. Chem.* **2000**, *72*, 4441−4446.

(5) Morris, R. B.; Franta, D. J.; White, H. S. *J. Phys. Chem.* **1987**, *91*, 3559−3564.

(6) Watkins, J. J.; Chen, J. Y.; White, H. S.; Abruna, H. D.; Maisonhaute, E.; Amatore, C. *Anal. Chem.* **2003**, *75*, 3962−3971.

(7) Smith, C. P.; White, H. S. *Anal. Chem.* **1993**, *65*, 3343−3353.

(8) Norton, J. D.; White, H. S.; Feldberg, S. W. *J. Phys. Chem* **1990**, *94*, 6772−6780.

(9) Slevin, C. J.; Gray, N. J.; Macpherson, J. V.; Webb, M. A.; Unwin, P. R. *Electrochem. Commun.* **1999**, *1*, 282−288.

(10) Shao, Y. H.; Mirkin, M. V.; Fish, G.; Kokotov, S.; Palanker, D.; Lewis, A. *Anal. Chem.* **1997**, *69*, 1627−1634.

(11) Penner, R. M.; Heben, M. J.; Longin, T. L.; Lewis, N. S. *Science* **1990**, *250*, 1118.

(12) Macpherson, J. V.; Unwin, P. R. *Anal. Chem.* **2000**, *72*, 276.

(13) Bach, C. E.; Nichols, R. J.; Meyer, H.; Besenhard, J. *Surf. Coat Technol.* **1994**, *67*, 139.

(14) Bach, C. E.; Nichols, R. J.; Beckmann, W.; Meyer, H.; Schulte, A.; Besenhard, J. O.; Jannkoudakis, P. D. *J. Electrochem. Soc.* **1993**, *140*, 1281.

(15) Sun, P.; Zhang, Z. Q.; Guo, J. D.; Shao, Y. H. *Anal. Chem.* **2001**, *73*, 5346−5351.

(16) Oldham, K. B.; Bond, A. M. *J. Electroanal. Chem.* **2001**, *508*, 28−40.

(17) Bard, A. J.; Faulker, L. R. *Electrochemical Methods*, 1st ed.; John Wiley: New York, 1980.

(18) Oldham, K. B. *J. Electroanal. Chem.* **1988**, *250*, 1.

(19) Amotore, C.; Fosset, B.; Bartlet, J.; Deakin, M. R.; Wightman, R. M. *J. Electroanal. Chem.* **1988**, *256*, 255.

(20) Bonnefont, A.; Argoul, F.; Bazant, M. Z. *J. Electroanal. Chem.* **2001**, *500*, 52.

(21) Murphy, W. D.; Manzanares, J. A.; Mafé, S.; Reiss, H. *J. Phys. Chem.* **1992**, *96*, 9983.

(22) Smyrl, W. H.; Eewman, J. S. *Trans. Faraday Soc.* **1966**, *62*, 207.

(23) Levich, B. *Dokl. Akad. Nauk SSSR* **1949**, *67*, 309.

(24) Mirkin, M. V.; Bard, A. J. *Anal. Chem.* **1992**, *64*, 2293−2302.

(25) Fawcett, W. R., Double Layer Effects in the Electrode Kinetics of Electron and Ion Transfer Reactions. In *Electrocatalysis*; Lipkowski, J., Ross, P. N., Eds.; Wiley-VCH: New York, 1998; p 322.

(26) Fawcett, W. R. *Can. J. Chem.* **1981**, *59*, 1844.

(27) Bockris, J. O. M.; Reddy, A. K. N. In *Modern Electrochemistry*; Plenum: New York, 1970; Vol. 2.

(28) Fawcett, W. R. *J. Electroanal. Chem.* **2001**, *500*, 264.